ChemPubSoc Europe

DOI: 10.1002/cctc.201601514

CHEMCATCHEM Full Papers

Towards the Broad Utilization of Gold Nanoparticles Entrapped in Organosilica

Rosaria Ciriminna,[a] Gabriele Scandura,[b] Valerica Pandarus,[c] Riccardo Delisi,[a] Antonino Scurria,[a] François Béland,[c] Giovanni Palmisano,[b] and Mario Pagliaro*[a]

SiliaCat Au, a nanoscale gold sol–gel hybrid material, was employed in the selective oxidation of alcohols under solvent-free conditions with oxygen as the primary oxidant. The catalyst is recyclable, and a thorough structural investigation, which included thermogravimetric analysis coupled to mass spectrometry, revealed structural details that will be useful in the development of new applications for this functional material to other areas of catalysis, analytical chemistry, bioimaging, and photonics.

Introduction

Alcohol oxidation catalyzed heterogeneously is a synthetic transformation used increasingly in industry for the clean synthesis of fine chemicals and or pharmaceuticals.[1] The interest is high, in particular, for solvent-free oxidation using O_2 or H_2O_2 as primary oxidants to make fine chemicals under mild reaction conditions with little or no waste generation,[2] in which the solid catalyst at the end of the reaction is separated easily from the reaction mixture and recycled or, even better, used in a flow microreactor in a continuous process.[3]

Among noble metal nanostructured catalysts developed in the last two decades, which include Pd nanocomposites for visible-light aerobic alcohol oxidation at room temperature,[4] supported Au nanoparticles are advantageous because they are not prone to leaching and poisoning caused by overoxidation or ligand chelation of the nanoparticles (NPs).[5] Furthermore, Au shows a low toxicity and is more abundant than platinum group metals (PGMs) used widely in catalysis.[6] In 2007, Stucky and Zheng reported that a trace amount of carbonate, borate, or acetate boosts the catalytic activity of supported Au NPs dramatically in the solvent-free oxidation of alcohols at 100 °C under 2 atm O_2.[7]

In general, electron-rich Au nanocrystallites loaded on reducible supports promote the adsorption and activation of O_2,[8] and recent successful efforts have been aimed to further improve the activity by the control of the support's Fermi level.[9] Recently, along with Ilharco and Fidalgo, we reported that SiliaCat Au, a hybrid material in which Au NPs are encapsulated within the inner mesopores of organosilica, is a suitable catalyst for the oxidation of several alcohols using Cao's biphasic oxidation protocol with H_2O_2 as the primary oxidant at 90 °C.[10] We ascribed the high activity of SiliaCat Au to the fact that the methyl groups in the organically modified silicate (ORMOSIL) matrix are not distributed uniformly but rather are concentrated at the external surface of the cages at which they lower the surface energy[11] and enhance the electron density at the surface of the entrapped Au NPs. In this work we show that SiliaCat Au under solvent-free conditions is more selective and active than the conventional Au/TiO_2 catalyst, at least for certain substrates. The catalyst, furthermore, is truly recyclable, which is a key requirement for a catalyst the active phase of which comprises precious Au, though used in a low catalytic amount.

Results and Discussion

The catalyst was active in the oxidative dehydrogenation of all alcohols tested, though with different activities (Table 1).

The activity and selectivity of SiliaCat Au in benzyl alcohol oxidation (entries 2 and 3) was significantly higher (93–94%) than that reported for the state-of-the-art Au/TiO_2 catalyst (55% selectivity at 35% conversion).[7] The conversion increases from 10 to 25% proportionally with the Au content (entries 2 and 3). A striking selectivity (99%) and good conversion (21%) were also obtained for cinnamyl alcohol (entry 7), a substrate that bears a conjugated double bond the aerobic oxidation (1 atm O_2, 160 °C) of which under solvent-free conditions over 5% Au/MnO_2 with 97% selectivity was reported in 2008.[12]

Secondary alcohol 1-phenylethanol (entry 6) was converted smoothly into the corresponding ketone with complete selectivity. The aliphatic primary alcohol 1-butanol was converted remarkably with 81% selectivity at 41% conversion into valued butyraldehyde (butanal), a chemical obtained in 6 million

[a] Dr. R. Ciriminna, Dr. R. Delisi, A. Scurria, Dr. M. Pagliaro
Istituto per lo Studio dei Materiali Nanostrutturati, CNR
via U. La Malfa 153
90146 Palermo (Italy)
E-mail: mario.pagliaro@cnr.it

[b] G. Scandura, Prof. G. Palmisano
Department of Chemical and Environmental Engineering
Masdar Institute of Science and Technology
PO BOX 54224, Abu Dhabi (United Arab Emirates)

[c] V. Pandarus, Dr. F. Béland
SiliCycle
2500 Parc-Technologique Blvd
Québec, G1P 4S6 (Canada)

Table 1. Results of the aerobic oxidation of alcohols[a] over SiliaCat Au[b] (promoter: K_2CO_3 1%).

Entry	Alcohol	Au [mol%]	Conversion after 5 h [%]	Aldehyde/ketone selectivity [%]
1	Benzyl alcohol	0.00	0.01	>99
2	Benzyl alcohol	0.02	10	94
3	Benzyl alcohol	0.05	25	93
4	1-Butanol	0.05	41	81
5	1-Octanol	0.05	11	21
6	1-Phenylethanol	0.05	36	>99
7	Cinnamyl alcohol	0.05	21	>99

[a] Reaction conditions: 10 mL alcohol, SiliaCat Au in the amount specified, 100 °C, 2 bar O_2, under stirring; [b] SiliaCat Au catalytic load = 0.086 mmol g^{-1}.

tonnes per year from propene hydroformylation. For comparison, the only product observed if we attempted the conversion of butanol over Au/TiO_2 is the ester.[7] Finally, both the yields and selectivity for 1-octanol conversion (entry 5) were low, which points to the poor interaction of the bulky C_8 alcohol with the Au NPs entrapped in the sol–gel cages.

To investigate the catalyst recyclability, the catalyst employed in benzyl alcohol oxidation was recovered by filtration, washed extensively with aqueous EtOH (50%), dried in an oven at 50 °C, and reused as such in a subsequent oxidation run with benzyl alcohol under the same conditions, and we took into account inevitable catalyst losses (≈90 mg per catalytic run). No reduction in activity or selectivity was observed in all five consecutive runs attempted.

We ascribe the high selectivity observed in benzyl alcohol oxidation to aldehyde to the hydrophobicity of the calcined ORMOSIL matrix, which prevents access to the sol–gel cage of the (hydrated) aldehyde molecules and subsequent further oxidation, whereas the presence of carbonate in an analogous solvent-free aerobic oxidation of benzyl alcohol over Au/TiO_2 rather benefits the formation of benzyl benzoate and even benzoic acid.[7] Indeed, although an uncalcined 10% methyl-modified ORMOSIL endows the matrix with a polarity that is still high and similar to that of methanol,[13] the cages of the SiliaCat Au matrix calcined at 250 °C contain a limited amount of Si–OH groups, which explains the limited reactivity of the uncalcined catalyst SiO_2-PVA-Au (PVA = polyvinyl alcohol).

SEM microphotographs of the blank support before and after calcination and of the SiliaCat Au catalyst before thermal treatment show that both the encapsulation of the Au nanoparticles as well as the calcination do not affect the morphology and amorphous structure of the organosilica matrix (Figure 1).

The TEM/scanning transmission electron microscopy (STEM)/energy-dispersive X-ray spectroscopy (EDS) analysis of the catalyst confirms the presence of Au NPs of a considerably larger size than <7–8 nm Au NPs used commonly in Au catalysis.[8] In detail, the organosilica matrix after calcination (SiO_2-PVA-Au-250) displays the Au NPs as dark grey/black nanospheres (Figure 2a) with a diameter of 14.4–52 nm. The STEM mode allows us to obtain a *z*-contrast image (Figure 2b) of the same sample and corroborates the radius of particles in the range 10.8–60 nm. In addition, we used EDS, in which the electron beam is focused onto a narrow spot (the STEM mode), to confirm that the small white features in the image are Au (Figure 3).

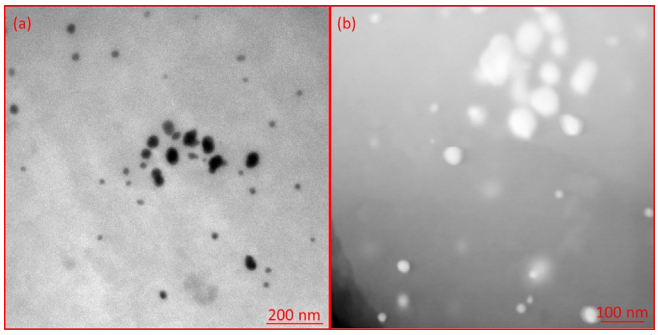

Figure 2. a) TEM and b) STEM images of SiO_2-PVA-Au-250.

The adsorption/desorption isotherms of SiliaCat Au catalyst series show a type IV hysteresis (Figure 4) and confirm that the newly synthesized materials are mesoporous.[1]

The BET isotherms offer a first clue that for the sol–gel-entrapped catalysts of the SiliaCat Au hydrothermal treatment with hot water at 90 °C under reflux is not effective to remove the PVA. Indeed, the catalysts before calcination have a considerably smaller surface area (Table 2), which increases only after calcination because of PVA degradation.

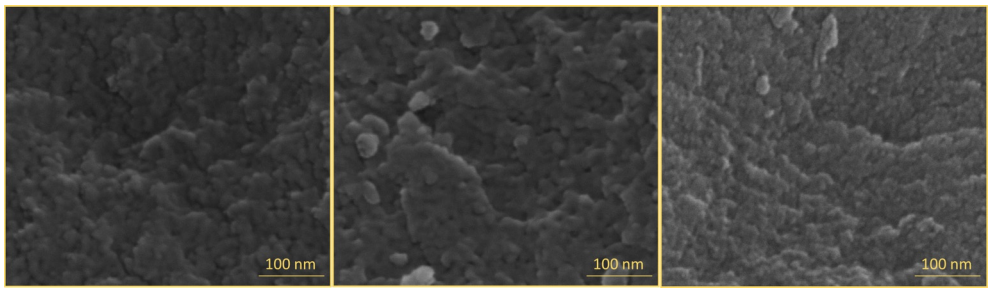

Figure 1. SEM images at 600 000× magnification of SiO_2-PVA (left), SiO_2-PVA-250 (center), and SiO_2-PVA-Au (right).

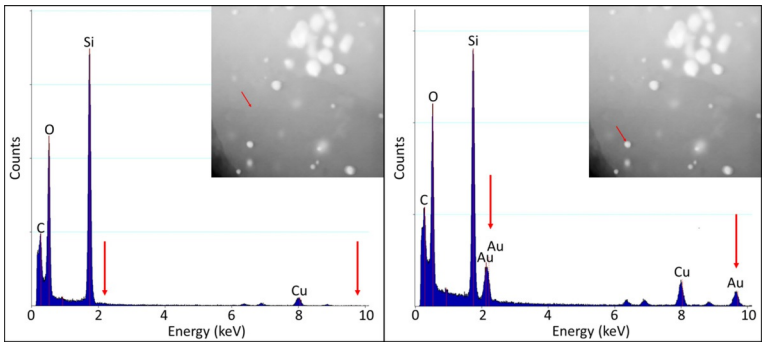

Figure 3. EDS spectra of SiO_2-PVA-Au-250. The red arrow in the insets shows the point at which the spectrum was obtained by working in STEM mode. The Cu peak is caused by the grid, whereas the C peak is caused by the grid and the sample.

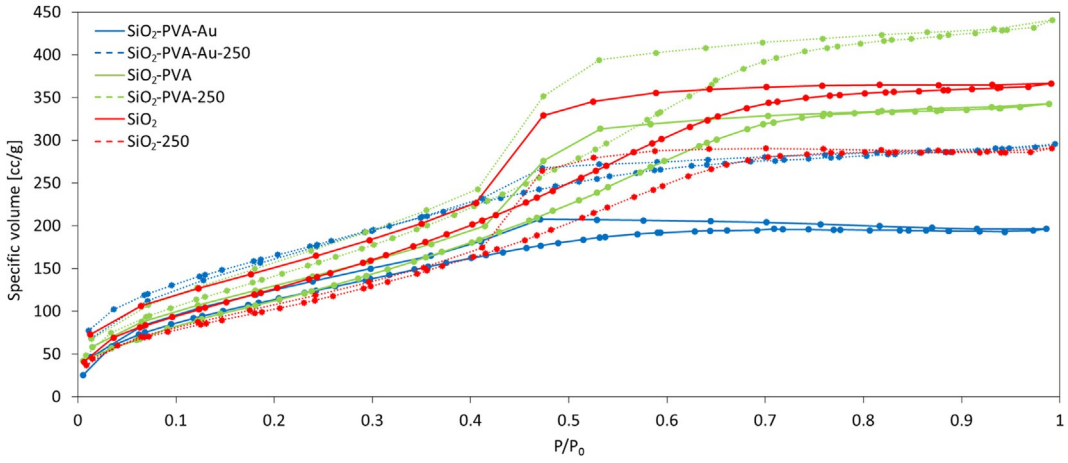

Figure 4. Adsorption–desorption isotherms of different samples.

Table 2. Structural properties of samples from N_2 adsorption–desorption isotherms.

Sample	Surface area (BET model) [$m^2 g^{-1}$]	Total pore volume [$cc g^{-1}$]	Surface area (BJH model) [$m^2 g^{-1}$]	Total pore volume (BJH model) [$cc g^{-1}$]
SiO_2-PVA-Au	481.0	0.583	149.9	0.431
SiO_2-PVA-Au-250	618.8	0.457	203.8	0.225
SiO_2-PVA	512.8	0.530	406.8	0.468
SiO_2-PVA-250	632.5	0.682	500.4	0.607
SiO_2	585.8	0.567	436.0	0.491
SiO_2-250	441.2	0.450	351.1	0.388

Conversely, the blank organosilica sample prepared without PVA (SiO_2) exhibits the regular behavior of a modestly alkylated ORMOSIL with a greatly reduced surface area after thermal treatment following the extensive condensation of the silanol groups at the surface of the sol–gel cage.[14]

The pore volume size distribution based on the Barrett–Joyner–Halenda (BJH) model shows that the encapsulation of Au NPs in the organosilica matrix results in both a reduced pore volume and a shift of the pore size distribution towards a smaller radius: an effect further enhanced by calcination at 250 °C (blue curves in Figure 5), and the differential volume for radius values under 40 Å increases after calcination because of the degradation of the PVA stabilizer.

The thermogravimetric analysis adds valuable information (Figure 6). The uncalcined samples show a fast weight loss during the first two segments of the heat ramp on reaching 120 °C (see below the MS analysis) because of the desorption of ethanol left in the cages after the sol–gel synthesis and that formed upon the hydrolysis of unreacted –Si(OEt) groups in the polycondensation between $Si(OEt)_4$ and $MeSi(OEt)_3$.

The calcined samples, in turn, show a much lower weight loss. For instance, the uncalcined blank organosilica (SiO_2) loses more weight than SiO_2-250 after 30 min (120 °C), after which the two curves are practically parallel to each other. On heating from 120 to 750 °C at 10 °C min^{-1} (third segment), the weight loss of different samples shows significant differences.

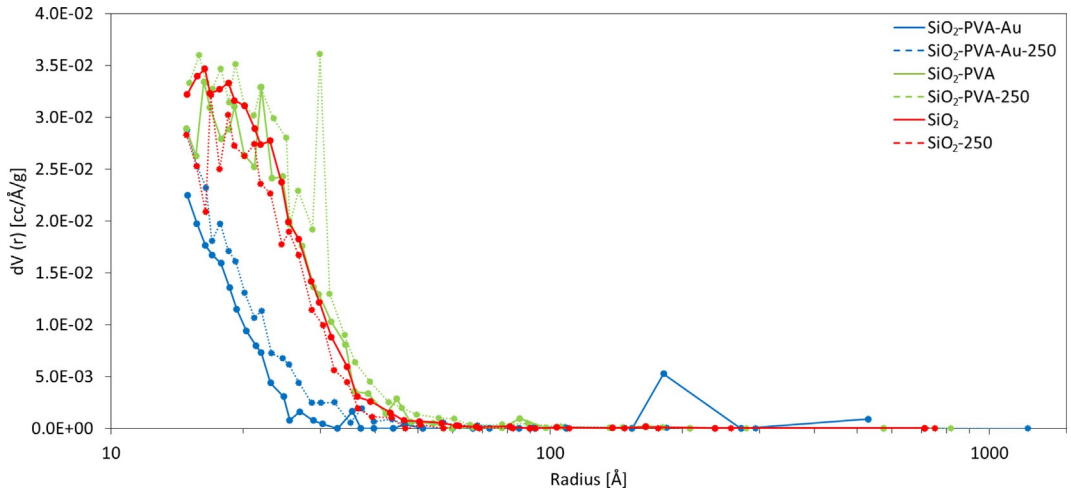

Figure 5. Pore radius distribution for different organosilica samples by using the BJH model.

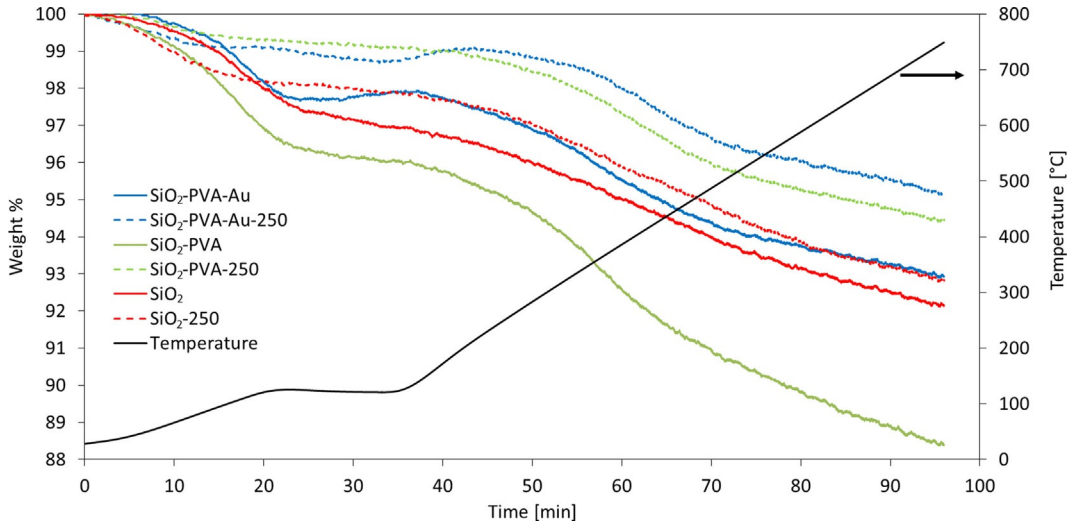

Figure 6. TG curves in He of different organosilica samples. The black curve shows the real temperature during the analysis.

Indeed, the difference amounts to just 0.68% for blank samples or calcined (SiO_2 and SiO_2-250) but it grows to 6.1% for the blank prepared in the presence of PVA before and after calcination (SiO_2-PVA and SiO_2-PVA-250). Finally, the smaller weight difference (2.2%) between SiO_2-PVA-Au and SiO_2-PVA-Au-250 is because the TGA experiment was performed by using the same amount (5 mg) of sample, which translates to a lower amount of PVA in the SiO_2-PVA-Au and SiO_2-PVA-Au-250 samples tested.

These results prove unequivocally that during the high-temperature thermal treatment at 250 °C the PVA molecules undergo degradation, as confirmed by subsequent TGA–MS analysis in which all peaks from $m/z = 10$ to 70 versus time were examined, even though only those relevant to this study are displayed in Figure 7.

The $m/z = 43$ signal versus time curve displayed in Figure 7a shows two peaks. The first one, within the second TGA segment (after 23 min, 120 °C), refers to the residual solvent traces (as explained previously). The signal at $m/z = 31$ is the base peak of the ethanol mass spectrum: the $m/z = 31$ signal versus time curve (not shown) shows a peak at the same time. Nonetheless ethanol has a distinctive $m/z = 43$ peak in its mass spectrum. The latter peak is more relevant in the plot shown in Figure 7a (≈63 min, 410 °C) because it appears only in samples that contain PVA, which shows evidence ("marker") of PVA degradation in these organosilica samples.

In detail, the blank organosilica sample prepared in the presence of PVA (SiO_2-PVA), which is the material with the highest notional PVA content, shows the most intense $m/z = 43$ peak followed by SiO_2-PVA-Au, which still records a conspicuous peak. The same peak for both samples after calcination (SiO_2-PVA-250 and SiO_2-PVA-Au-250) is significantly less intense and it is very weak for in the spectrum of SiO_2-PVA-Au-250. The difference in the intensity of the peak at $m/z = 43$ between the pairs SiO_2-PVA/SiO_2-PVA-250 and SiO_2-PVA-Au/SiO_2-PVA-Au-250 is in perfect agreement with the difference in the percent weight loss after the third segment of the TGA.

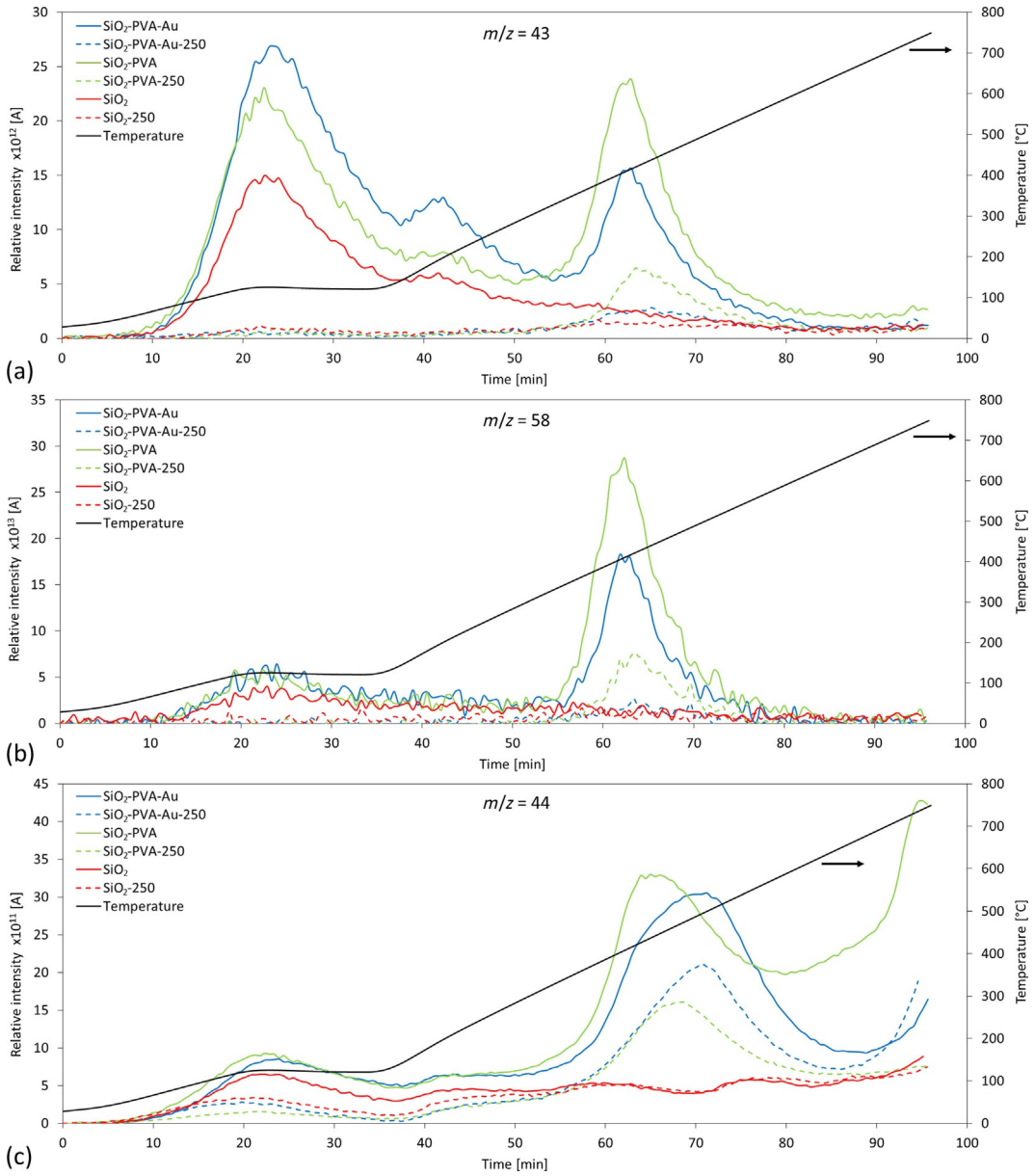

Figure 7. Current relative intensity of a) $m/z = 43$, b) 58, and c) 44 of different organosilica samples. The temperature curve refers to the real temperature of the TG analysis (Figure 6). Relative intensity is current intensity at time t minus current intensity at time 0.

The $m/z = 58$ signal versus time curve presented in Figure 7b exhibits the same two peaks as $m/z = 43$. Nevertheless, the first one (23 min, 120 °C) is extremely faint and can be ascribed to impurities in the reactants used during the catalyst preparation (which disappear in the calcined samples). The second peak at 63 min (410 °C) is identical to that shown by the $m/z = 43$ signal. One of the compounds yielded from the thermal degradation of PVA is acetone, the base peak of which is at $m/z = 43$ in the mass spectrum and the second greatest peak is at $m/z = 58$. During the calcination at 250 °C, the PVA present in the sol–gel composite undergoes partial degradation, and acetone is one of the degradation products, in agreement with the degradation mechanism of PVA/silica nanocomposites reported by Peng and Kong.[15]

The last signal at $m/z = 44$ (Figure 7c) is the base peak of CO_2, namely, the mineralization product of the organic compounds. The most intense peak, once again related to PVA only (samples SiO_2 and SiO_2-250 do not show this peak), is observed after approximately 71 min (500 °C) for SiO_2-PVA-Au and SiO_2-PVA-Au-250, 68 min (465 °C) for SiO_2-PVA-250, and 65 min (440 °C) for SiO_2-PVA. These peaks are shifted in time with respect to those at $m/z = 43$ and 58 (especially for samples that contain Au), that is, they are not caused by the same chemical of the $m/z = 43$ and 58 peaks but may rather be attributed to the thermal mineralization of acetone and other products of PVA thermal degradation such as acetic acid (the base peak of which is exactly $m/z = 43$) and acetaldehyde, which are other products formed from the thermal degradation of PVA.[13] What

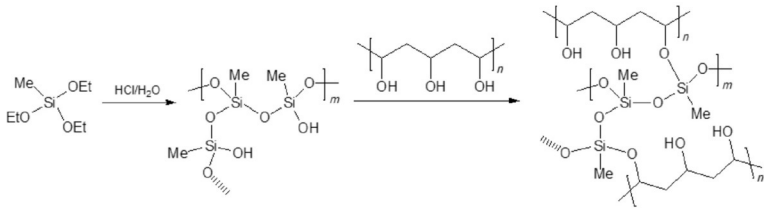

Scheme 1. Condensation reaction between PVA and silicon ethoxides in the sol–gel synthesis of SiliaCat Au.

is relevant here, and confirms the partial degradation of PVA during the calcination step of the catalyst preparation, is that the intensity of these peaks for the calcined samples (SiO_2-PVA-250 and SiO_2-PVA-Au-250) is again much smaller than that of SiO_2-PVA and SiO_2-PVA-Au.

First described by Nakane and co-workers in 1996 (who aimed to prepare water-permselective membranes or immobilization carriers for biocatalysts),[16] PVA-silica hybrid composites form cross-linked networks through the condensation of hydrolyzed silanes in the sol with the hydroxyl groups in the PVA backbone (Scheme 1).

Usually, silica/PVA composites with PVA amounts >20% show two distinct weight-loss stages,[17] one at around 375 °C that reflects the decomposition of PVA side chain and another at 450 °C caused by the decomposition of the polymer main chain. In our case, the amount of PVA in SiliaCat Au is much lower than 20% and the thermal treatment at 250 °C, though crucially important to enhance the catalytic activity of the material, removes most PVA molecules, especially those at the outer surface of the sol–gel cages as shown by the increase in the surface are and pore size reduction of the catalyst before and after the treatment, though not all PVA (the ether bond in the composite formed during preparation is particularly strong).

What is unique to SiliaCat Au prepared in the presence of PVA is that, because of the pronounced physical and chemical stabilization of the entrapped Au nanocrystallites caused by the sol–gel cage, the high-temperature thermal treatment for ligand removal, which in conventional catalysts obtained by colloidal deposition of the support leads generally to a significant increase in the size (and morphology change) of the NPs and worsens their catalytic activity,[18,19] increases the catalytic activity by removing most of the PVA with no substantial change in the morphology and size of the Au NPs.

Conclusions

Heterogeneous Au catalysts are already applied in the manufacture of bulk chemicals in the petrochemical industry.[20] En route to the practical application of heterogeneous Au nanocatalysts to fine chemicals and pharmaceuticals manufacturing, we report the SiliaCat Au catalyst that comprises 5% methyl-modified silica that encapsulates Au nanoparticles (NPs) of a relatively large size to mediate the solvent-free aerobic oxidation of alcohols selectively under mild conditions (100 °C, 2 atm O_2) in the presence of carbonate as promoter, which adds to recent successful results on alcohol oxidation with H_2O_2 following Cao's protocol.[21] Compared to the conventional Au/TiO_2 catalyst, SiliaCat Au is more active and selective for benzyl and cinnamyl alcohol and affords a high yield of valued aldehydes, such as butanal through the oxidation of the corresponding primary alcohol butan-1-ol. The catalyst is stable and recyclable, and a detailed thermogravimetric analysis with MS investigation shows evidence that the thermal treatment of the catalyst at 250 °C is enough to remove most of the polyvinyl alcohol used as a ligandstabilizer during the sol–gel synthesis without affecting the size and the morphology of the encapsulated Au NPs protected within the sol–gel cages that comprise the inner porosity of the glassy catalyst. These findings are also important in light of the forthcoming application of this new material the active phase of which is made of relatively large Au NPs (of lower toxicity than smaller Au NPs)[22] to different applicative domains from photonics[23] and analytical chemistry[24] to bioimaging.[25]

Experimental Section

The synthetic procedure to afford SiliaCat Au in three steps has been reported elsewhere.[10] All catalysts studied in the present work are newly synthesized 5% methyl-modified silicas of the AuRC1 series (Table 3). The sol–gel synthesis starts from silicon alkoxides $Si(OEt)_4$ and $MeSi(OEt)_3$ in the presence of chloroauric acid, and PVA is used as a stabilizing ligand to prevent the sintering of colloidal Au^0 nanoparticles. All materials synthesized have undergone a first hydrothermal treatment that consists of the treatment of the material with hot water at 90 °C under reflux, which has been shown to be effective to remove all PVA used as a ligand-stabilizer in the case of Au/TiO_2.[26]

Table 3. Blank and catalytic ORMOSILs of the AuRC1 series investigated in this study.

Sample	Features
SiO_2-PVA-Au	AuRC1c not calcined
SiO_2-PVA-Au-250	AuRC1c calcined @250 °C
SiO_2-PVA	Blank+PVA not calcined
SiO_2-PVA-250	Blank+PVA calcined @250 °C
SiO_2	Blank not calcined
SiO_2-250	Blank calcined @250 °C

The SiliaCat Au catalyst used in the catalytic tests is a sample obtained after further thermal treatment at 250 °C in air for 4 h (SiO_2-

PVA-Au-250). Its catalytic load (0.086 $mmol_{Au}\,g^{-1}$) was assessed by using inductively coupled plasma mass spectrometry (ICP-MS).

Catalytic tests

Aliphatic, aromatic, primary, and secondary alcohols were used as representative substrates. All the experiments were conducted in a 15 mL Parr batch reactor controlled by using a thermostat at 100 °C under 2 bar O_2 atmosphere. In certain experiments, the consumption of oxygen with a consequent reduction in pressure required us to replenish the O_2 consumed. The reactor contained alcohol substrate (10 mL), SiliaCat Au (0.02 and 0.05 % mol), and K_2CO_3 (1 mol %). The autoclave was closed and charged with oxygen through a valve. The reactor was heated to 100 °C, and the reaction mixture was stirred for 5 h. The reaction products were analyzed by using GC by using a Shimadzu GC-17 chromatograph equipped with a Supelcowax column.

Structural analyses

SEM images were recorded by using a FEI Nova NanoSEM 650 microscope. TEM, STEM, and EDS analyses were obtained by using a Tecnai F20 X-Twin FEG transmission electron microscope operated at 200 kV equipped with EDAX and HAADF detectors. Samples were prepared by suspending the powders in 2-propanol followed by sonication. Finally, 2 μL of the suspension was dropped three times on a 300 mesh copper grid provided by Ted Pella (Redding, California), and the solvent was evaporated at RT.

The adsorption/desorption isotherms were measured by using a Quantachrome NOVA 2000e surface area and pore size analyzer using N_2 as adsorbent. Before the analysis, the samples were degassed under vacuum at 200 °C for 4 h for the samples calcined at 250 °C and at 60 °C for 20 h and for the noncalcined samples. Specific surface areas were determined by using the multipoint BET method as an average of desorption values in the low pressure range ($P/P_0 = 0$–0.35). The adsorption curve in the whole range of pressure was fitted with the Barrett–Joyner–Halenda (BJH) model to assess the pore size distribution.

All samples were characterized by using TGA–MS. A Netzsch STA 449 F3 thermal analysis equipment was used for the TGA. In detail, 5 mg of the powdered material kept under He flow (15 $mL\,min^{-1}$) was heated from 30 to 120 °C at a rate of 5 °C min^{-1} (first segment), further maintained at 120 °C for 15 min (second segment), and finally heated from 120 to 750 °C at a rate of 10 °C min^{-1} (third segment). The exit gas from the TGA was examined by using a Netzsch QMS 403 D mass spectrometer. The intensity current versus time curves were collected for all *m/z* from 10 to 70. The same TGA–MS experiment was performed with no sample as a control. The discussion of the MS results makes reference to the MS spectra of chemicals available online at the NIST Chemistry WebBook (http://webbook.nist.gov/chemistry). Characterization of samples that contain Au was performed by using powders with a fixed Au loading of 0.05 %.

Acknowledgements

This article is dedicated to Dr Les Edye, head of research at Leaf Resources (Australia), almost 20 years after his memorable visit to Sicily, for all he has done to advance carbohydrate and glycerol chemistry in the context of the bioeconomy.

Conflict of interest

The authors declare no conflict of interest.

Keywords: alcohols · gold · oxidation · sol–gel processes · supported catalysts

[1] R. Ciriminna, V. Pandarus, F. Béland, Y.-J. Xu, M. Pagliaro, *Org. Process Res. Dev.* **2015**, *19*, 1554.
[2] M. Morad, M. Sankar, E. Cao, E. Nowicka, T. E. Davies, P. J. Miedziak, D. J. Morgan, D. W. Knight, D. Bethell, A. Gavriilidis, G. J. Hutchings, *Catal. Sci. Technol.* **2014**, *4*, 3120.
[3] P. L. Alsters, Aerobic (Alcohol) Oxidation in Flow, *Organic Process Research & Development*, Barcelona, 28 – 30 September **2015**.
[4] N. Zhang, S.i. Liu, X. Fu, Y.-J. Xu, *J. Phys. Chem. C* **2011**, *115*, 22901.
[5] T. Mallat, A. Baiker, *Chem. Rev.* **2004**, *104*, 3037.
[6] X. Liu, L. He, Y.-M. Liu, Y. Cao, *Acc. Chem. Res.* **2014**, *47*, 793 – 804.
[7] N. Zheng, G. D. Stucky, *Chem. Commun.* **2007**, 3862.
[8] C. Della Pina, E. Falletta, M. Rossi, *Chem. Soc. Rev.* **2012**, *41*, 350.
[9] S.-i. Naya, M. Teranishi, R. Aoki, H. Tada, *J. Phys. Chem. C* **2016**, *120*, 12440.
[10] R. Ciriminna, A. Fidalgo, V. Pandarus, F. Béland, L. M. Ilharco, M. Pagliaro, *ChemCatChem* **2015**, *7*, 254.
[11] M. Pagliaro, R. Ciriminna, M. W. C. Man, S. Campestrini, *J. Phys. Chem. B* **2006**, *110*, 1976.
[12] L.-C. Wang, L. He, Q. Liu, Y.-M. Liu, M. Chen, Y. Cao, H.-Y. He, K.-N. Fan, *Appl. Catal. A* **2008**, *344*, 150.
[13] C. Rottman, G. Grader, D. Avnir, *Chem. Mater.* **2001**, *13*, 3631.
[14] J. Yang, J. Chen, J. Song, *Vib. Spectrosc.* **2009**, *50*, 178.
[15] Z. Peng, L. X. Kong, *Polym. Degrad. Stab.* **2007**, *92*, 1061 – 1071.
[16] F. Suzuki, K. Nakane, J.-S. Piao, *J. Mater. Sci.* **1996**, *31*, 1335 – 1340.
[17] K. Nakane, T. Yamashita, K. Iwakura, F. Suzuki, *J. Appl. Polym. Sci.* **1999**, *74*, 133 – 138.
[18] H. Yin, C. Wang, H. Zhu, S. H. Overbury, S. Sun, S. Dai, *Chem. Commun.* **2008**, 4357 – 4359.
[19] L. Wen, J.-K. Fu, P.-Y. Gu, B.-X. Yao, Z.-H. Lin, J.-Z. Zhou, *Appl. Catal. B* **2008**, *79*, 402 – 409.
[20] R. Ciriminna, C. Della Pina, E. Falletta, J. H. Teles, M. Pagliaro, *Angew. Chem. Int. Ed.* **2016**, *55*, 14210; *Angew. Chem.* **2016**, *128*, 14420.
[21] R. Ciriminna, V. Pandarus, R. Delisi, A. Scurria, F. Giordano, M. P. Casaletto, F. Béland, M. Pagliaro, *Chem. Cent. J.* **2016**, *10*, 61.
[22] I. Fratoddi, I. Venditti, C. Cametti, M. V. Russo, *Toxicol. Res.* **2015**, *4*, 796 – 800.
[23] S. Eustis, M. A. El-Sayed, *Chem. Soc. Rev.* **2006**, *35*, 209 – 217.
[24] *Gold Nanoparticles in Analytical. Chemistry Vol. 66,* M. Valcárcel, A. I. López-Lorente (Eds), Elsevier, Amsterdam: 2014.
[25] P. K. Jain, K. S. Lee, I. H. El-Sayed, M. A. El-Sayed, *J. Phys. Chem. B* **2006**, *110*, 7238 – 7248.
[26] J. A. Lopez-Sanchez, N. Dimitratos, C. Hammond, G. L. Brett, L. Kesavan, S. White, P. Miedziak, R. Tiruvalam, R. L. Jenkins, A. F. Carley, D. Knight, C. J. Kiely, G. J. Hutchings, *Nat. Chem.* **2011**, *3*, 551.

Manuscript received: November 25, 2016
Revised: January 18, 2017
Accepted Article published: January 19, 2017
Final Article published: March 15, 2017